Microstructure evolution and hardening mechanism of 18Cr2Ni4WA steel during combined carburized and carbonitrided treatment

Xiaojun Yang[a], Ke Chen[b], Yuedong Yuan[a], Qiyuan Chen[*b], Lei Wang[a], Xiaonan Wang[*b], Chao Li[a], Liyuan Zhao[a], Ye Pu[a]
[a]Changshu Tiandi Coal Machinery Equipment Co., Ltd., Suzhou, 215500, China
[b]School of Iron and Steel, Soochow University, Suzhou, 215021, China
[*] Corresponding author: qychen1992@suda.edu.cn; wxn@suda.edu.cn

ABSTRACT

Microstructure evolution and hardening mechanism of 18Cr2Ni4WA steel subjected to combined high-temperature carburizing, two high-temperature tempering, carbonitriding, quenching, low-temperature treatment, and low-temperature tempering heat treatment were investigated in this study. The effect of surface precipitation phases and retained austenite on surface hardness after different heat treatments was studied throughout the process. The results indicated that the combined treatment converted the lath martensite (LM) surface layer into acicular martensite (AM), carbide and residual austenite (RA). Furthermore, subzero treatment led to the improvement of mechanical properties through the reduction of residual austenite and the increase of carbide. The deformation of the martensite lattice and the compressive stress within the retained austenite are reduced through low-temperature tempering, which led to a decrease in austenite stability, facilitating its transformation into martensite. This study deepens the current understanding of the hardening mechanism of 18Cr2Ni4WA steel during carburizing carbonitriding composite heat treatment, providing a theoretical basis and experimental basis for expanding its application fields.

Keywords: 18Cr2Ni4WA steel, carburizing carbonitriding, hardness, subzero treatment, low-temperature tempering

1. INTRODUCTION

Owing to its high strength, toughness and hardenability, 18Cr2Ni4WA steel is used to manufacture high-speed and heavy-duty Marine engines, aeroengines, gears, drive shafts and other key components [1-4]. The hardenability and tempering stability of 18Cr2Ni4WA steel are improved by high alloying elements such as Cr and Ni. However, in carburizing and carbonitriding, the microstructure evolution and hardening mechanism are complex and critical, which affects the product quality.

The carburization and nitridation of steel improve the hardness and wear resistance by introducing C and N into surface layer, which also modifies the mechanical properties. By carburizing, the C content of the surface layer is increased, and the high hardness martensite structure is obtained by quenching. But for 18Cr2Ni4WA steel, there are a lot of RA in the carburizing layer besides martensite. These RA affect the hardness and mechanical properties during subsequent heat treatment processes. By carbonitriding, the C and N content of the surface layer is increased, and the hardness and wear resistance of the steel are improved, but the hardening mechanism remains to be further studied.

In summary, the study of microstructure evolution and hardening mechanism of 18Cr2Ni4WA steel in the combined carburized and carbonitrided treatment is of great significance for optimizing the heat treatment process and improving the mechanical properties. A combination of experimental and theoretical analysis was chosen in this paper to reveal the microstructure transformation of 18Cr2Ni4WA steel during the combined carburized and carbonitrided treatment. The hardening mechanism of 18Cr2Ni4WA steel was studied. This will provide theoretical basis and technical support for practical production.

2. EXPERIMENTAL MATERIALS AND METHODS

A Φ50 mm × L 40 mm annealed 18Cr2Ni4WA steel was used in this study, whose chemical composition is listed in table 1. Gas carburizing of the sample was carried out in a pit-type carburizing furnace (RQD-90-9), followed by strong carburizing (carbon potential 1.25 wt.%) at 950 ℃, diffusion stage (carbon potential 0.85 wt.%) at the same temperature for 46 h. After carburizing, high temperature tempering, carbonitriding, quenching, subzero treatment, and low

International Conference on Automation and Intelligent Technology (ICAIT 2024), edited by R. Usubamatov, S. Feng, X. Mei,
Proc. of SPIE Vol. 13401, 134010P · © The Authors. Published under a Creative Commons Attribution CC-BY 3.0 License
doi: 10.1117/12.3051031

temperature tempering are carried out successively. In carbonitriding, the carbon potential in the strong osmotic and diffusion stage is 0.9 wt.% and 0.75 wt.%, respectively. The ammonia flow rate is 4 L/min. To prevent decarbonization during heat treatment, the entire process is protected with nitrogen. The heat treatment process flow chart is shown in figure 1.

Table 1. Chemical compositions of 18Cr2Ni4WA steel (wt.%).

Element	C	Cr	Ni	W	Mn	Si	Fe
Content	0.14	1.45	4.14	0.79	0.46	0.24	Bal.

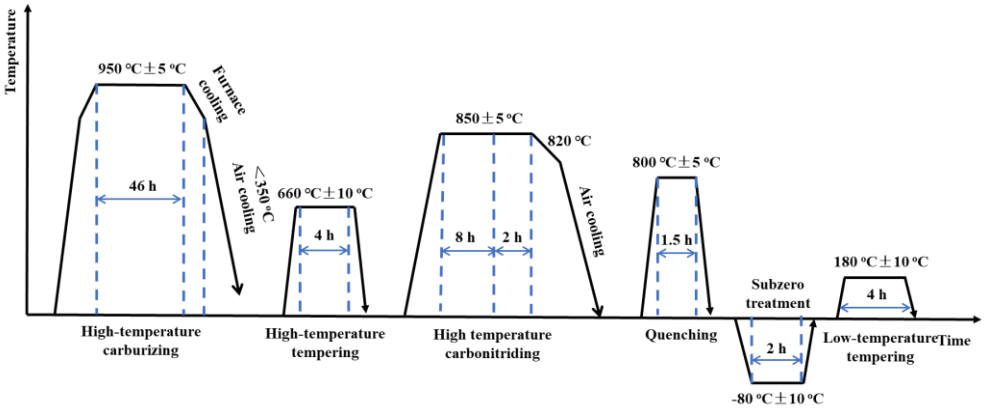

Figure 1. Combined carburized and carbonitrided treatment.

Metallographic samples are prepared using conventional preparation processes, including grinding, polishing, and etching. Subsequently, the RX50M optical microscope and SU5000 scanning electron microscope were used to observe the microstructure of the carburized layer. The RA volume fraction was measured by X-ray diffraction (XRD, SmartLab 9kW) with a sample size of 10 mm×10 mm×2 mm. Cu Kα radiation is used. The scanning speed and Angle are 2 °/min and 40~100 °, respectively. The voltage and current are 40 kV and 150 mA respectively. In order to obtain the volume fraction of RA, the Eq.(1) was used [5]:

$$V_{\mathrm{A}} = \frac{1-V_{\mathrm{C}}}{1+G\frac{I_{\mathrm{M(hkl)_i}}}{I_{\mathrm{A(hkl)_j}}}} \tag{1}$$

Where V_A is the volume fraction of RA in steel; V_C is the volume fraction of total carbides in steel; I_M is the cumulative intensity of the diffraction lines from the martensitic crystal faces in steel; I_A is the cumulative intensity of the diffraction lines from the austenitic crystal faces in steel; G the ratio of austenite crystal faces to the intensity correlation factor corresponding to the martensite crystal faces. The G values of different diffraction pairs are 2.46, 1.32, 1.78, 1.21, 0.65, and 0.87, respectively. Each G value is brought into Eq. (1) and finally V_A is calculated.

The microhardness test is performed on the MH-500 Vickers microhardness tester. The load used is 10 N and residence time is 10 s. The distance between the hardness test points is 0.5 mm to ensure that the distance between each other is far enough to avoid unnecessary interference caused by local strain hardening of adjacent indentation. Each microhardness was the average of 5 measurements.

3. RESULTS

The microstructure of the base material (BM) is shown in figure 2, which is basically martensite. The SEM images of carburized sample are shown in figure 3. The microstructure of the infiltration layer is acicular martensite, and no carbide exists. The microstructures of the core are AM and LM. This is caused by the lower C content in the center of the sample than in the carburized layer. This on the one hand leads to the core AM grain size is coarse, on the other hand leads to the formation of LM. The SEM images of quenched sample are shown in figure 4. The microstructure after quenching is AM + LM + RA. RA is distributed at martensite grain boundaries.

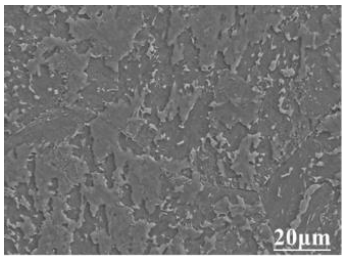

Figure 2. Microstructure of the BM.

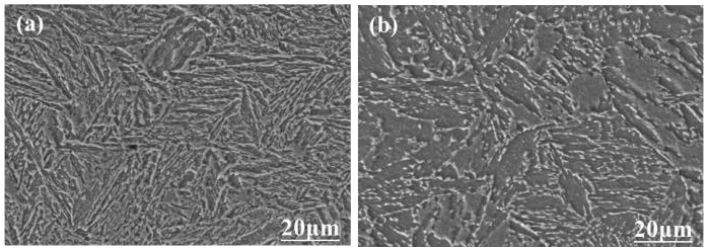

Figure 3. SEM images of the microstructure after carburizing: (a) surface; (b) core.

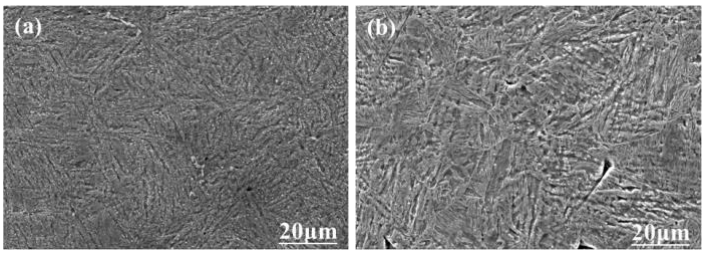

Figure 4. SEM images of microstructure after quenching: (a) surface; (b) core.

XRD results of the sample after combined carburized and carbonitrided treatment are shown in figure 5. The sampling position is 0.5mm away from the sample surface. The results show that martensite and austenite are detected. The strongest XRD peaks are assigned to the martensitic (110) crystal plane, and no carbide peaks are observed. The results of XRD are consistent with those of SEM morphology. The RA volume fraction is 36.3%.

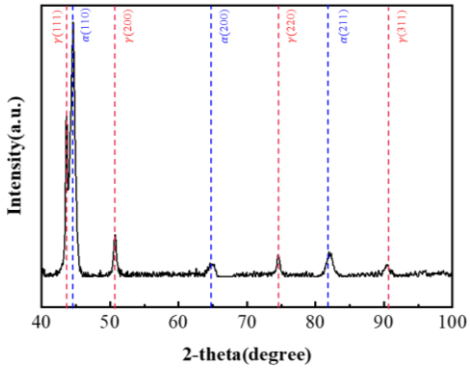

Figure 5. XRD pattern of the hardened layer at a depth of 0.5 mm.

The hardness gradient of the hardened layer is shown in figure 6. According to the Chinese national standard GB/T 9450-2005 [6], the hardened layer produced by carburizing quenching is defined as the vertical distance from the surface to the depth of Vickers hardness of 550 HV. As shown in figure 6, the depth of hardened layer is 4.2 mm. The maximum hardness is located on the sample surface, with a hardness value of 742 HV. The hardness of the core is 438 HV. This hardness gap is due to the gradual reduction of C content.

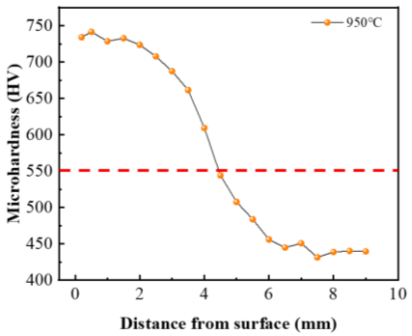

Figure 6. Hardness gradient of the hardened layer.

4. DISCUSSION

4.1 Effect of subzero treatment on microstructure and surface hardness

A subzero treatment (-80 ℃) is introduced between quenching and low tempering. The effect of subzero treatment on microstructure and properties is studied. The SEM images of subzero treatment sample are shown in figure 7. The surface microstructure of the sample is AM and carbide. The core microstructure of the sample is LM and carbide. The content of carbide in the surface microstructure is obviously higher than that in the core microstructure. There is no obvious change in the microstructure of the infiltration layer between the subzero treatment sample and the quenched sample. RA is distributed in martensitic grain boundaries.

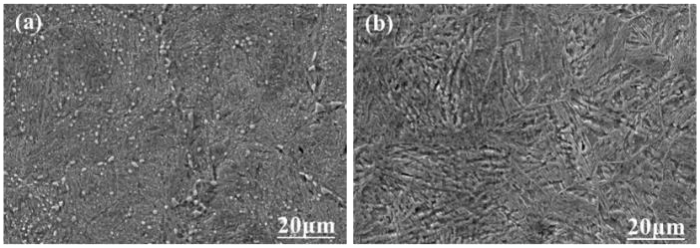

Figure 7. SEM images of microstructure after subzero treatment: (a) surface; (b) core.

XRD results of the sample after subzero treatment are shown in Figure 8. The sampling position is 0.5 mm away from the sample surface. The RA volume fraction is 10.2 %.

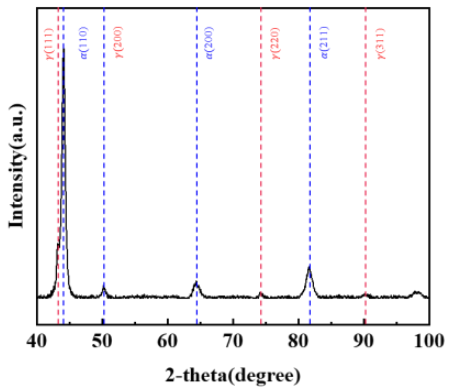

Figure 8. XRD pattern of the hardened layer at a depth of 0.5 mm after subzero treatment.

The hardness gradient of the infiltration layer is shown in figure 9. The maximum hardness is located on the sample surface, with a hardness value of 781 HV. The hardness of the core is 440 HV. The effective hardened layer depth is 4.2 mm. After subzero treatment, the hardened layer depth is not changed significantly, but the hardness is increased significantly. This is because the RA content is reduced and the C content is increased [7, 8].

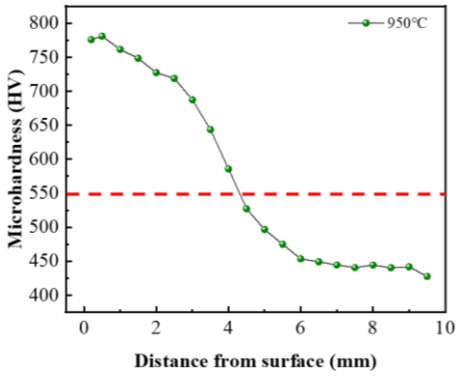

Figure 9. Hardness gradient of infiltration layer after low temperature treatment.

4.2 Effect of low tempering on microstructure and surface hardness

The SEM images of low tempering sample are shown in figure 10. The microstructure of the surface and core are mainly AM and LM, respectively. What can be observed is that low tempering leads to carbide precipitation. T after quenching is mainly AM + LM + RA. Subzero treatment resulted in the reduction of massive RA. After low tempering, the microstructure is martensite + RA + carbide. XRD results of the sample after low tempering are shown in figure 11. The RA volume fraction is 9.5%.

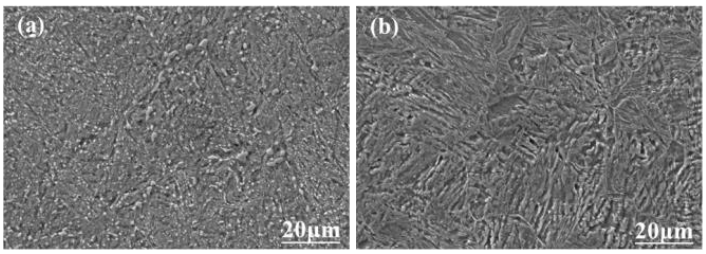

Figure 10. SEM images of low tempering microstructure: (a) surface; (b) core.

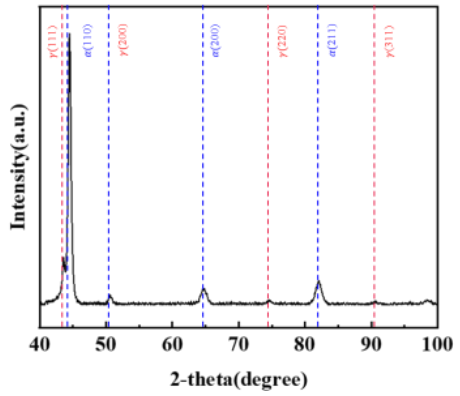

Figure 11. XRD pattern of the hardened layer at a depth of 0.5 mm after low temperature tempering.

The hardness gradient of the infiltration layer is shown in figure 12. The maximum hardness is located on the sample surface, with a hardness value of 752 HV. The hardness of the core is 440 HV. The effective hardening layer depth is 4.2 mm. The hardness is higher than the sample after quenching. Quenched martensite contains unsaturated solid solution carbon, and there is a certain residual stress. At the same time, high C content leads to lower M_S points. The martensite phase transition during quenching is relatively late and incomplete, resulting in more residual austenite. The result is obvious hardness lowering and softening of the hardened layer. In contrast, Low tempering increases hardness by reducing martensitic lattice deformation, reducing residual stress, reducing residual austenite stability and promoting martensitic transformation.

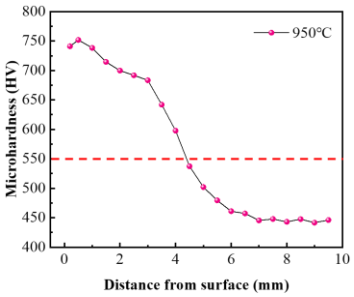

Figure 12. Hardness gradient of infiltration layer after low tempering.

5. CONCLUSIONS

(a) After carburizing and quenching, the surface and core matrix structure are AM and LM, respectively. From the surface to the core, the hardness gradually decreases.

(b) After subzero treatment, the content of RA decreased from 36.3% to 10.2% after quenching. The transformation of RA to martensite is promoted, thus effectively improving the microhardness.

(c) The transformation of RA is effectively promoted by low tempering. This is because the deformation of the martensite lattice is reduced, the residual stress is reduced, and the residual austenite stability is reduced.

ACKNOWLEDGMENTS

This work was supported by the National Key R&D Program of China [Grant No. 2023YFB3408000], and the Natural Science Foundation of the Jiangsu Higher Education Institutions of China [Grant No. 24KJB430021].

REFERENCES

[1] L. Li, L. Sun, Experimental and numerical investigations of crack behavior and life prediction of 18Cr2Ni4WA steel subjected to repeated impact loading, Engineering Failure Analysis, 65 (2016) 11-25.
[2] C.B. Xia, M.W. Tu, Q.J.J.A.M.R. Pan, Performance and property of Ni base coatings by using plasma arc technology for 18Cr2Ni4WA steel repairing, Advanced Materials Research, 189 (2011) 311-315.
[3] J. Yang, K. Pang, Elastoplastic behavior of case-carburized 18Cr2Ni4WA steel by indenter testing, Journal of Aerospace Engineering, 32 (2019) 04019045.
[4] H. Mohrbacher, Metallurgical concepts for optimized processing and properties of carburizing steel, Advances in Manufacturing, 4 (2016) 105-114.
[5] Z.H. Wu, Z.X. Li, Q.Y. Zhang, Y. Jiang, Z.G. Liu, Y.D. Yuan, Y. Xue, X.N. Wang, Effect of microstructure on wear resistance during high temperature carburization heat treatment of heavy-duty gear steel, Materials Today Communications, 40 (2024) 109486.
[6] Steels—Determination and verification of the depth of carburized and hardened cases, GB/T 9450-2005, The General Administration of Quality Supervision, Inspection and Quarantine of the People's Republic of China (AQSIQ): Beijing, 2005.
[7] Y. Yan, Z. Luo, K. Liu, C. Zhang, M. Wang, X. Wang, Effect of cryogenic treatment on the microstructure and wear resistance of 17Cr2Ni2MoVNb carburizing gear steel, Coatings, 12 (2022) 281.
[8] L. Song, X. Gu, F. Sun, J. Hu, Reduced internal oxidation by a rapid carburizing technology enhanced by pre-oxidation for 18CrNiMo7-6 gear steel, Vacuum, 160 (2019) 210-212.